A Non-Conforming Generalization of Raviart-Thomas Elements to the Spherical Harmonic Even-Parity Neutron Transport Equation

S. Van Criekingen

A Non-Conforming Generalization of Raviart-Thomas Elements to the Spherical Harmonic Form of the Even-Parity Neutron Transport Equation

S. Van Criekingen

Commissariat à l'énergie atomique (CEA-Saclay),
DEN/DM2S/SERMA/LENR (Bât 470)
91191 Gif-sur-Yvette Cedex, France
serge.van-criekingen@cea.fr

Abstract

The Raviart-Thomas finite elements provide an appropriate spatial discretization of the mixed-dual form of the diffusion equation. This discretization can then be coupled to an efficient solution method. The high performances achieved by such an approach triggered research on its possible generalization to the transport equation using a spherical harmonic (or P_N) angular approximation. In view of the difficulty of developing a straightforward generalization within the mixed-dual framework, we here consider 2-D non-conforming (i.e., allowing interface discontinuities) finite elements coupled to the second-order form of the transport equation. This non-conforming approach keeps the mixed-dual property of the relaxation of the flux interface continuity constraint. We investigate different non-conforming elements and compare them to the well-known Lagrangian conforming elements.

Key words: neutron transport, spherical harmonics, Raviart-Thomas finite elements, non-conforming finite elements

1 Introduction

The Raviart-Thomas (RT) finite elements (Raviart and Thomas 1977) are known to be appropriate for the discretization of the mixed-dual formulation of the diffusion equation. In this formulation, two unknowns, namely the scalar flux and the vector current, are simultaneously evaluated. The simplicity of the diffusion equation enables the implementation of very efficient solution methods. This is done (among others) in the MINOS solver (Baudron and

Lautard 2005). In this solver, the flux is expressed in terms of the current and eliminated from the linear system. The resulting system is then solved for the current using an efficient alternate direction implicit (ADI) approach. The flux can then be recovered from the current values. This approach proved to be very efficient. Notably, several benchmarks can be treated using only one directional sweeping (in the ADI process) per outer iteration. This makes the computing time roughly proportional to the number of nodes. The MINOS solver also provides a simplified transport (SP_N) approximation, since this approximation amounts to solving a set of diffusion equations.

The success of the MINOS solver triggered research on how to possibly generalize it to the transport equation using a spherical harmonic (or P_N) angular approximation (Fedon-Magnaud et al. 1995; Wu 1996; Van Criekingen et al. 2006; Van Criekingen 2004). No method could so far achieve this in a simple way, that is using the RT mixed-dual elements - or an extension thereof - for the spatial discretization. The difficulty here stems from the fact that the RT elements are not directly applicable to the common setting of the transport mixed formulation, i.e., the one based on the even/odd (angular) parity decomposition introduced by Vladimirov (1963). Indeed, this decomposition yields two scalar unknowns, namely the even and odd part of the angular flux, while the RT elements simultaneously approximate a scalar and a vector unknown (scalar flux and vector current in the diffusion case).

In an attempt to circumvent this problem, we here introduce a vector unknown based on the even/odd parity decomposition into the mixed-dual transport formulation. Then, in view of the deficiency of such an approach, we turn our attention to a second-order (also known as standard) primal alternative, using non-conforming finite elements. While the use of the second-order formulation with P_N approximation is well-known with Lagrangian elements (de Oliveira 1986), its use with non-conforming elements is to the best of our knowledge not documented in the literature.

Several authors established equivalences between mixed schemes such as RT, and non-conforming approaches based on the second-order formulation. This was done by Hennart in the nuclear engineering community (Hennart 1986; Hennart and del Valle 1993). But numerical analysts also established such equivalences for quite general second-order problems (Arnold and Brezzi 1985; Arbogast and Chen 1995). The proof of such equivalences are hard to generalize to the transport case given the increased complexity of the equation compared to the diffusion one. In this paper no such generalizations have been attempted. Moreover, although theoretically interesting, these equivalences are not profitable at an implementation level, i.e., we can not simply re-use a mixed RT solver turning it into a non-conforming second-order one. However, an important issue remains, that is that non-conforming approaches, similarly to the mixed-dual one, relax the interface continuity constraint on

the flux. The flexibility and parallelization capabilities of the non-conforming finite elements have proved useful in other fields (Kloucek et al. 1996; Ha et al. 2002).

The paper is organized as follows. In Section 2 a review is given of the RT mixed-dual method as applied to the diffusion case. In Section 3, we describe our attempt at applying the RT elements to P_N transport while keeping a mixed-dual formulation. In Section 4, we first adapt Hennart's approach (Hennart 1986) to P_N transport and define a family of 2-D non-conforming finite elements. We then further simplify the lowest-order of these elements to yield a four node non-conforming element. Section 5 is devoted to criticality calculations performed with the non-conforming elements which were investigated in Section 4, and a comparison is made with the classical Lagrangian conforming elements. Finally, concluding remarks can be found in Section 6.

2 Raviart-Thomas elements for the diffusion equation

Recall that diffusion theory yields the coupled pair of first order equations

$$\boldsymbol{\nabla} \cdot \boldsymbol{J}(\boldsymbol{r}) + \sigma_r(\boldsymbol{r})\, \phi(\boldsymbol{r}) = s(\boldsymbol{r}) \tag{1}$$

$$\boldsymbol{\nabla}\phi(\boldsymbol{r}) + 3\sigma(\boldsymbol{r})\boldsymbol{J}(\boldsymbol{r}) = 0 \tag{2}$$

where the two unknowns are the scalar flux $\phi(\boldsymbol{r})$ and the vector current $\boldsymbol{J}(\boldsymbol{r})$. As is well-known, introducing test functions and applying the divergence theorem to (2) yields a mixed-dual weak form (Lautard et al. 1999). In any mixed method, the finite-dimensional approximation spaces for the two unknowns cannot be chosen independently. This well-posedness requirement arises from the "Ladyshenskaya-Babuška-Brezzi" (or "inf-sup") condition (e.g. Roberts and Thomas 1991). It can be shown (Raviart and Thomas 1977) that this condition is satisfied if the flux approximation space S_ϕ equals the divergence of the current approximation space $S_{\boldsymbol{J}}$, that is

$$\boldsymbol{\nabla} \cdot S_{\boldsymbol{J}} = S_\phi. \tag{3}$$

This requirement is met by the RT elements (Raviart and Thomas 1977). Indeed, at order k, the RT_k element on a rectangular reference unit finite element uses the following spaces

$$S_{\boldsymbol{J}} = \{\boldsymbol{J} = j_x \mathbf{1}_x + j_y \mathbf{1}_y,\ j_x \in Q_{k+1,k} \text{ and } \ j_y \in Q_{k,k+1}\}, \qquad S_\phi = Q_{k,k}, \tag{4}$$

where the polynomial space $Q_{a,b}$ is defined by

$$Q_{a,b} = \{x^i y^j,\ 0 \le i \le a,\ 0 \le j \le b\}.$$

Pascal triangles in figure 1 illustrate the polynomials present in the current ((a) and (b)) and flux (c) basis for the RT element of order 1 (i.e., RT_1). Comparing (a) and (b) to (c) shows that condition (3) is verified for RT_1. The degrees of freedom are taken to be $k+1$ values of $\boldsymbol{n}\cdot\boldsymbol{J}$ on each rectangle side, and $(k+1)^2$ values of ϕ inside the element. The RT elements enforce the continuity of $\boldsymbol{n}\cdot\boldsymbol{J}$, but allow interface discontinuities for ϕ.

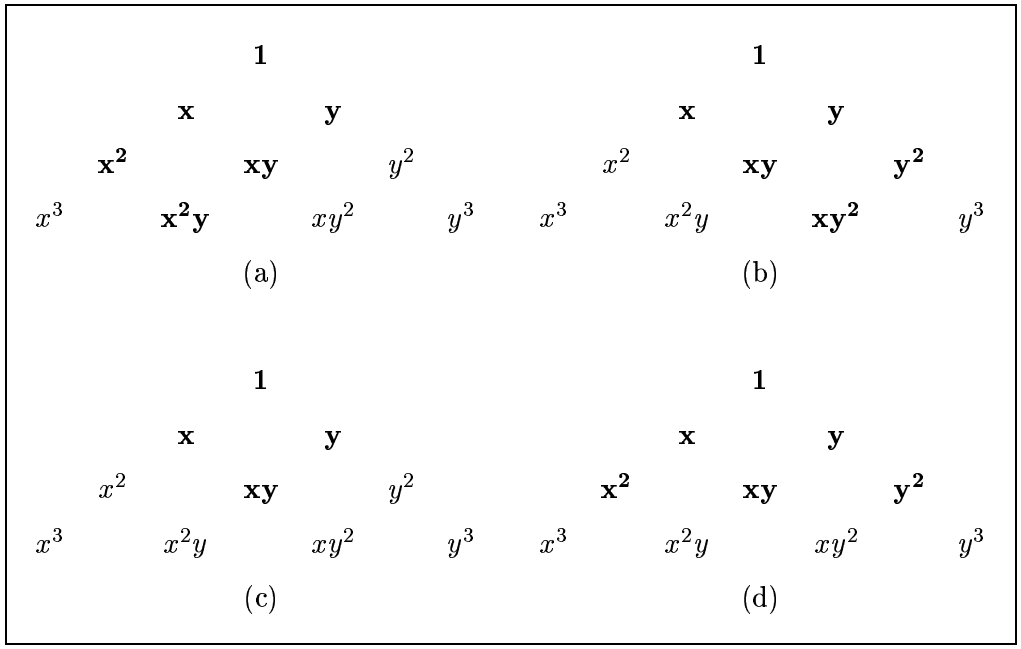

Fig. 1. Mixed Dual RT_1 finite element: in boldface, terms present in the approximation space for the vector unknown $x-$ (a) and $y-$ (b) components, and for the scalar unknown (c); in (d), extension of the scalar unknown approximation space that accounts for the crossed terms appearing in the transport case.

3 Attempts at mixed-dual P_N transport

3.1 Looking for a mixed-dual formulation

The even/odd angular parity decomposition of the angular flux $\Psi(\boldsymbol{r},\boldsymbol{\Omega})$ defines its even component Ψ^+ and its odd component Ψ^- according to

$$\Psi^{\pm}(\boldsymbol{r},\boldsymbol{\Omega}) = \frac{1}{2}\left(\Psi(\boldsymbol{r},\boldsymbol{\Omega}) \pm \Psi(\boldsymbol{r},-\boldsymbol{\Omega})\right).$$

With these definitions, the transport equation can be written as the coupled pair of first order equations

$$\boldsymbol{\Omega}\cdot\boldsymbol{\nabla}\Psi^-(\boldsymbol{r},\boldsymbol{\Omega})+\sigma(\boldsymbol{r})\,\Psi^+(\boldsymbol{r},\boldsymbol{\Omega})=\sigma_s(\boldsymbol{r})\,\phi(\boldsymbol{r})+s(\boldsymbol{r}) \tag{5}$$

$$\boldsymbol{\Omega}\cdot\boldsymbol{\nabla}\Psi^+(\boldsymbol{r},\boldsymbol{\Omega})+\sigma(\boldsymbol{r})\,\Psi^-(\boldsymbol{r},\boldsymbol{\Omega})=0 \tag{6}$$

where for simplicity we assumed isotropic scattering and sources, and with $\phi(\boldsymbol{r})=\int_{4\pi}d\Omega\Psi^+(\boldsymbol{r},\boldsymbol{\Omega})$ the scalar flux.

The most straightforward way to obtain a mixed-dual form for (5) and (6) uses two scalar unknowns, namely Ψ^+ and Ψ^- (Fedon-Magnaud et al. 1995; Wu 1996). This way is thus not appropriate for RT elements. Moreover, the increase in the number of unknowns should then be compensated by a better conditioning of the resulting system matrix, which has not been proved so far. This is even more true for mixed-hybrid methods based on (5) and (6) (Van Criekingen et al. 2006), since such methods use additional interface unknowns (which can be interpreted as a Lagrange multipliers) to enforce interface continuity constraints.

In order to obtain a scalar and a vector unknown, we introduce (assuming as in the remainder of this paper that $\sigma\neq 0$)

$$\boldsymbol{p}(\boldsymbol{r},\boldsymbol{\Omega})=-\frac{1}{\sigma}\,\boldsymbol{\nabla}\Psi^+(\boldsymbol{r},\boldsymbol{\Omega}). \tag{7}$$

With this definition, equation (6) becomes $\Psi^-=\boldsymbol{\Omega}\cdot\boldsymbol{p}$ and we are lead to the coupled pair of equations

$$\boldsymbol{\Omega}\cdot\boldsymbol{\nabla}\,(\boldsymbol{\Omega}\cdot\boldsymbol{p})+\sigma\,\Psi^+=\sigma_s\int_{4\pi}\Psi^+\,d\Omega+s \tag{8}$$

$$\boldsymbol{p}+\frac{1}{\sigma}\,\boldsymbol{\nabla}\Psi^+=0. \tag{9}$$

Then, introducing test functions $\tilde{\Psi}^+$ and $\tilde{\boldsymbol{p}}$ in (8) and (9), respectively, integrating over space (V is the spatial domain, and ∂V its boundary) and angle, and applying the divergence theorem to the second equation, we obtain

$$\int_{4\pi}\int_V\left(\tilde{\Psi}^+\,\boldsymbol{\Omega}\cdot\boldsymbol{\nabla}\,(\boldsymbol{\Omega}\cdot\boldsymbol{p})+\sigma\,\tilde{\Psi}^+\,\Psi^+-\sigma_s\tilde{\Psi}^+\int_{4\pi}\Psi^+\,d\Omega'\right)d\Omega\,dV = \int_{4\pi}\int_V\tilde{\Psi}^+ s\;d\Omega\,dV \tag{10}$$

$$\int_{4\pi}\int_V\left(\sigma\tilde{\boldsymbol{p}}\boldsymbol{p}-\boldsymbol{\nabla}\cdot\tilde{\boldsymbol{p}}\,\Psi^+\right)d\Omega\,dV+\int_{4\pi}\int_{\partial V}\boldsymbol{n}\cdot\tilde{\boldsymbol{p}}\,\Psi^+\,d\Omega\,dS=0. \tag{11}$$

This is the mixed-dual weak form with unknowns Ψ^+ and $\boldsymbol{p}$, for which we can now consider a RT-type discretization.

Again since we use a mixed formulation, the finite-dimensional approximation spaces for the two unknowns cannot be chosen independently. Letting $S_{\boldsymbol{p}}$ and

S_{Ψ^+} respectively denote the approximation spaces for $\boldsymbol{p}$ and Ψ^+, an analogy with the classical diffusion analysis suggests that the equivalent of condition (3) in our transport case is

$$\boldsymbol{\Omega} \cdot \boldsymbol{\nabla} (\boldsymbol{\Omega} \cdot S_{\boldsymbol{p}}) = S_{\Psi^+},$$

since the divergence operator in (1) is replaced by the more involved operator $\boldsymbol{\Omega} \cdot \boldsymbol{\nabla} (\boldsymbol{\Omega} \cdot)$ in (8). Note that we have for any $\boldsymbol{p} = p_x \mathbf{1}_x + p_y \mathbf{1}_y \in S_{\boldsymbol{p}}$,

$$\boldsymbol{\Omega} \cdot \boldsymbol{\nabla} (\boldsymbol{\Omega} \cdot \boldsymbol{p}) = \Omega_x^2 \, \partial_x p_x + \Omega_x \Omega_y \, \partial_x p_y + \Omega_x \Omega_y \, \partial_y p_x + \Omega_y^2 \, \partial_y p_y.$$

The presence of "crossed terms" $\partial_x p_y$ and $\partial_y p_x$ in this last expression (not present in the simple divergence of (3)) forbids the use of the RT elements as such. Rather than look for a hypothetical transport formulation that avoids such crossed terms, one can broaden S_{Ψ^+} so as to take these terms into account. In this view, figure 1 (d) presents an extension of the RT_1 scalar approximation space which accounts for the crossed terms.

Introducing angular dependence, we therefore consider the approximation space defined at order k by

$$\begin{aligned} S_{\boldsymbol{p}} &= \{\boldsymbol{p} = p_x \mathbf{1}_x + p_y \mathbf{1}_y, \; p_x \in Y_e \otimes Q_{k+1,k} \text{ and } p_y \in Y_e \otimes Q_{k,k+1}\}, \\ S_{\Psi^+} &= Y_e \otimes P_{k+1} \end{aligned}$$

where the polynomial space P_a is defined by

$$P_a = \{x^i y^j, \; 0 \leq i + j \leq a\} \tag{12}$$

and Y_e contains the even-parity spherical harmonics. Thus the spatial part of the vector space $S_{\boldsymbol{p}}$ is the same as $S_{\boldsymbol{J}}$ in the diffusion case (cf. (4)), while the spatial part of the scalar space S_{Ψ^+} has been extended. One can notice that our heuristic approach makes this extension relevant only for RT_k with $k \geq 1$.

Substituting the above expansions into equations (10) and (11) yields a non-symmetric form of matrix equations, which means that the mixed-dual formulation considered here is not self-adjoint.

3.2 A fixed-source test problem

We now introduce a demanding fixed-source test problem in order to test the above formulation. This problem, depicted in figure 2, is derived from the Azmy benchmark (Azmy 1987). Since the latter is correctly treated by the SP_N method, a low-density region was added so as to make the SP_N method fail. Figure 3 illustrates the deficiency of the SP_N method (line of circles)

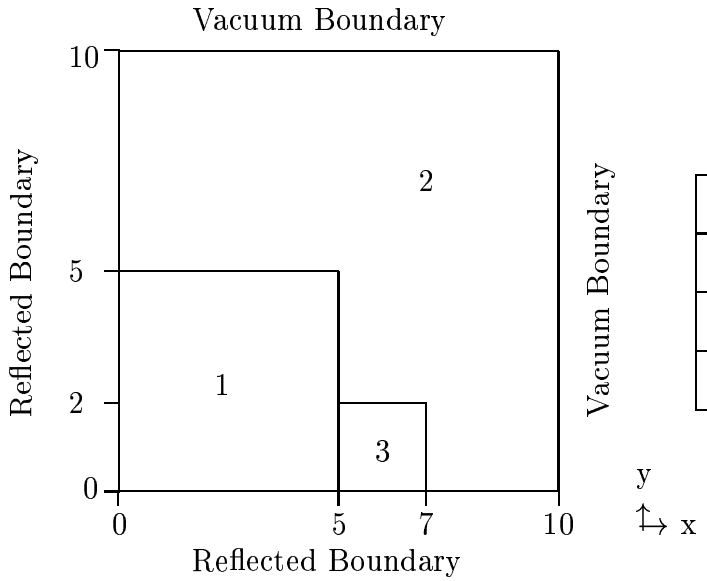

zone	σ	σ_s	s
1	1	0.5	1
2	2	0.1	0
3	0.1	0.05	0

Fig. 2. Our fixed-source test problem ($\sigma_{(s)}$ per unit length, s per unit volume).

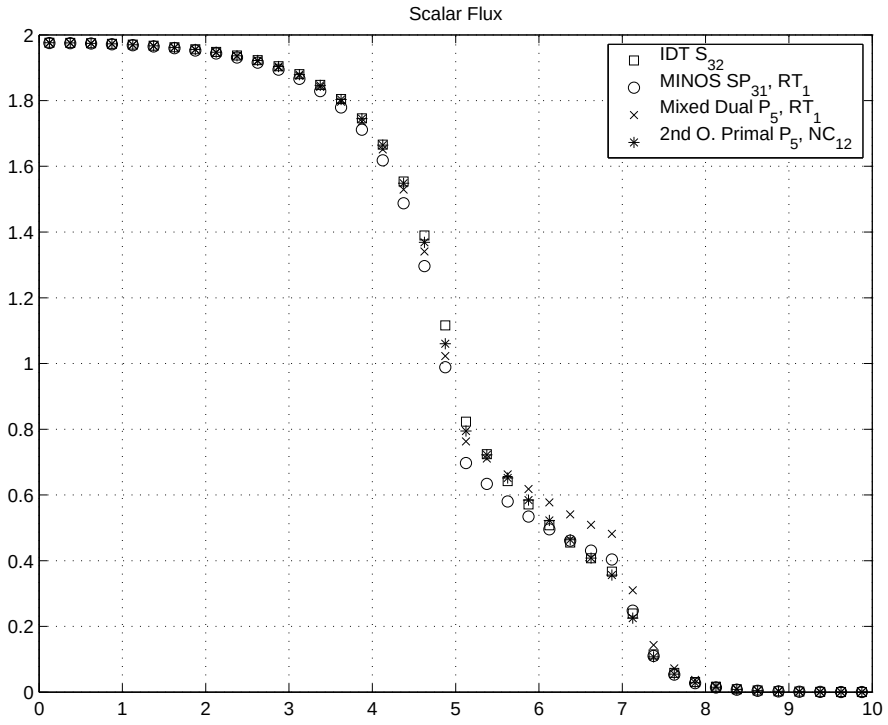

Fig. 3. Cell-averaged scalar flux along the line of mesh cells centered at $y = 1.125$ for our fixed-source test problem.

compared to a reference solution (line of squares) obtained with the discrete ordinate solver IDT of the APOLLO2 code (Zmijarevic 1999). A 40×40 grid was employed in all our test calculations.

Unfortunately, the approach proposed in Section 3.1 proved unsatisfactory on our test problem, as illustrated in figure 3 (line of "x"). Besides, the extension of the scalar approximation space did not prove helpful in practice. In fact, examining the discretized weak form, it can be shown that the additional spatial expansion functions in S_{Ψ^+} (compared to S_ϕ) do not contribute to the cell-averaged value of the scalar flux. Our numerical tests moreover showed that these additional expansion functions bring a randomly oscillating contribution to the solution in the low-density region (i.e., for $x \in [5, 7]$).

3.3 Other attempts

The deficiency of this approach can be thought to be due (at least in part) to a too tight continuity requirement on $\boldsymbol{p}$: the RT discretization yields a vector with continuous normal component across interfaces, while this is in general not physically true for $\boldsymbol{p}$. Therefore, we developed another mixed-dual formulation redefining our vector unknown as $\boldsymbol{p} = -\frac{1}{\sigma}\,\boldsymbol{\Omega}\,(\boldsymbol{\Omega}\cdot\boldsymbol{\nabla}\Psi^+) = \boldsymbol{\Omega}\,\Psi^-$, whose normal component is physically continuous across interfaces. However, this approach also failed to provide acceptable results on our test problem, probably because in this case the directional constraint on the discretized vector $\boldsymbol{p}$ is too loose. In fact, this last formulation yields a system of matrix equations which is the transpose of the one obtained with the first definition of $\boldsymbol{p}$ (equation (7)) , but this property could not be exploited to obtain an improved method.

Finally, we explored the possibility of using the self-adjoint angular flux (SAAF) equation of Morel and McGhee (1999) rather than the even/odd-parity decomposition (Cartier 2005b). Defining as vector unknown (Cartier 2005a) $\boldsymbol{p}(\boldsymbol{r},\boldsymbol{\Omega}) = -\frac{1}{\sigma}\,\boldsymbol{\Omega}\,\boldsymbol{\Omega}\cdot\boldsymbol{\nabla}\Psi(\boldsymbol{r},\boldsymbol{\Omega})$, one obtains using the SAAF

$$\begin{aligned}
&\boldsymbol{\nabla}\cdot\boldsymbol{\Omega}\,\boldsymbol{\Omega}\cdot\boldsymbol{p}(\boldsymbol{r},\boldsymbol{\Omega}) + \sigma(\boldsymbol{r})\,\Psi(\boldsymbol{r},\boldsymbol{\Omega}) = \\
&\quad \sigma_s(\boldsymbol{r})\int_S \Psi(\boldsymbol{r},\boldsymbol{\Omega})\,d\Omega + s(\boldsymbol{r}) - \boldsymbol{\nabla}\cdot\frac{1}{\sigma(\boldsymbol{r})}\boldsymbol{\Omega}\left(\sigma_s(\boldsymbol{r})\int_S \Psi(\boldsymbol{r},\boldsymbol{\Omega})\,d\Omega + s(\boldsymbol{r})\right) \\
&\boldsymbol{\Omega}\,\boldsymbol{\Omega}\cdot\boldsymbol{\nabla}\Psi(\boldsymbol{r},\boldsymbol{\Omega}) + \sigma(\boldsymbol{r})\,\boldsymbol{p}(\boldsymbol{r},\boldsymbol{\Omega}) = 0
\end{aligned}$$

This yields a symmetric system of matrix equations. With this formulation, the P_N approximation expands the angular dependence of the two unknowns Ψ and $\boldsymbol{p}$ using the same complete set of spherical harmonics up to order N. The problem here is that the lowest-order angular approximation, which expands the angular part of Ψ and $\boldsymbol{p}$ using the spherical harmonics up to order 1 (i.e. Y_{00}, Y_{10} and $Y_{1\pm1}$) does not correspond to the diffusion equation. This fact seems to impair the possibility of building a P_N transport method on this basis.

4 A Non-Conforming Second-Order Alternative

The well-known even-parity (or primal) second-order formulation (de Oliveira 1986; Palmiotti et al. 1995) is obtained by expressing Ψ^- in terms of Ψ^+ in equation (6), and substituting the result into equation (5). Note that the second-order primal weak form can in fact be derived without using any second-order derivative (that is why the terminology "standard" is sometimes preferred to "second-order"). Indeed, multiplying equation (5) by a test function $\tilde{\Psi}^+$, and integrating over space and angle yields

$$\int_{4\pi}\int_V \tilde{\Psi}^+ \left(\mathbf{\Omega}\cdot\boldsymbol{\nabla}\Psi^- + \sigma\Psi^+ - \sigma_s \int_{4\pi} d\Omega' \Psi^+ \right) d\Omega\, dV = \int_{4\pi}\int_V s\, \tilde{\Psi}^+\, d\Omega\, dV$$

Integrating by parts (with respect to $\boldsymbol{r}$), we obtain

$$\begin{aligned} &-\int_{4\pi}\int_V \Psi^- \mathbf{\Omega}\cdot\boldsymbol{\nabla}\tilde{\Psi}^+\, d\Omega\, dV + \int_{4\pi}\int_{\partial V} \mathbf{\Omega}\cdot\boldsymbol{n}\tilde{\Psi}^+\Psi^-\, d\Omega\, dS \\ &\quad + \int_{4\pi}\int_V \left(\sigma\tilde{\Psi}^+\Psi^+ - \sigma_s\tilde{\Psi}^+ \int_{4\pi}\Psi^+ \right) d\Omega\, dV = \int_{4\pi}\int_V s\, \tilde{\Psi}^+\, d\Omega\, dV. \end{aligned}$$

Expressing Ψ^- in terms of Ψ^+ using (6) finally yields the weak form

$$\begin{aligned} &\int_{4\pi}\int_V \mathbf{\Omega}\cdot\boldsymbol{\nabla}\tilde{\Psi}^+ \frac{1}{\sigma}\mathbf{\Omega}\cdot\boldsymbol{\nabla}\Psi^+\, d\Omega\, dV + \int_{4\pi}\int_{\partial V} \mathbf{\Omega}\cdot\boldsymbol{n}\tilde{\Psi}^+\Psi^-\, d\Omega\, dS \\ &+ \int_{4\pi}\int_V \left(\sigma\tilde{\Psi}^+\Psi^+ - \sigma_s\tilde{\Psi}^+ \int_S \Psi^+ \right) d\Omega\, dV = \int_{4\pi}\int_V s\, \tilde{\Psi}^+\, d\Omega\, dV. \end{aligned} \tag{13}$$

The Ψ^- term in the surface integral (second term) of this last expression is expressed in terms of Ψ^+ through the boundary conditions. The unique unknown in this case is thus Ψ^+.

The above formulation is well-known, and lies for instance at the basis of the transport production code EVENT (de Oliveira 1986). However, while this code uses the usual Lagrangian finite elements (as described in R.T.Ackroyd 1997, for instance), we here consider non-conforming finite elements. By "non-conforming", we mean elements that allow interface discontinuities for Ψ^+. Recall that the mixed-dual *RT* finite elements enforce the continuity of the normal component of the vector unknown, but allow interface discontinuities for the scalar unknown. This relaxation property is thus kept intact when using non-conforming elements. In fact, equivalences between mixed and non-conforming second-order methods can be established. This has been done in the (nuclear) engineering community by Hennart (Hennart and del Valle 1993), as well as in the numerical analysis community at a more general level (Arnold and Brezzi 1985; Arbogast and Chen 1995).

In the diffusion case, Hennart (1986) introduced a family of non-conforming nodal schemes based on the second-order primal formulation of the equation, using the scalar flux as a unique unknown. The word "nodal" here means that Hennart took the degrees of freedom to be edge or cell moments, while the classical finite element approach considers point values as degrees of freedom. The polynomial expansions in Hennart's approach are defined at order k so that the unique spatial approximation space is spanned by

$$Q_{k+2,k} \cup Q_{k,k+2} \qquad k = 0, 1, 2, \ldots . \tag{14}$$

Pascal triangles in figure 4 (a) and (b) illustrate this for the lowest two spatial expansion orders, $k = 0$ and $k = 1$. The degrees of freedom are then $k + 1$ moments on each edge of a rectangular element, and $(k+1)^2$ cell moments on the interior of the element. Note that this repartition of unknowns between the interior and the edge of a rectangular element is the same as in the RT elements. This further illustrates the relationship between these non-conforming elements and the original RT ones. Note by the way that these nodal schemes, later applied to the transport equation using discrete ordinates for the angular discretization (del Valle and Mund 2004), are still denoted by "RT_k" even though they do not apply to a mixed-dual formulation.

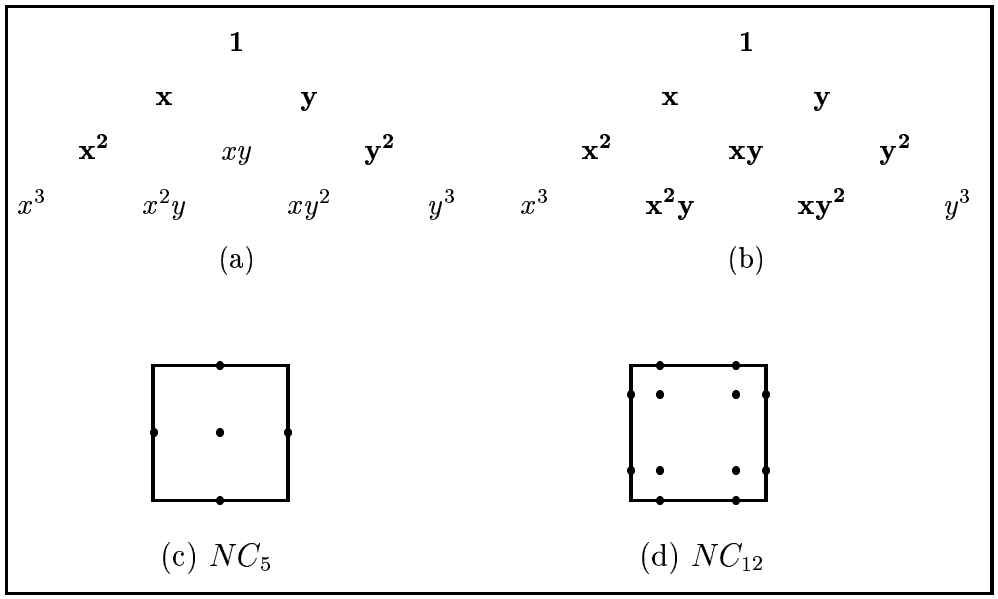

Fig. 4. Second-order primal version of the RT_0 (a) and RT_1 (b) elements: in boldface, terms present in the approximation space for the unique unknown; position of the nodes in the proposed element of order 0 (c) and 1 (d).

Hennart's approach is adapted to the primal form of the second-order neutron transport equation with a spherical harmonic angular approximation by defining a family of 2-D non-conforming finite elements. We keep the spatial approximation spaces defined in (14), but not the "nodal" character of the

method: we here use node point values as unknowns. We choose to locate these nodes at Gauss points. In general at order k, the Ψ^+ spatial approximation space is thus again spanned by $Q_{k+2,k} \cup Q_{k,k+2}$, but the degrees of freedom are now the Ψ^+ point values at the $k+1$ Gauss points on each edge, and at the $(k+1)^2$ interior Gauss points within each element. This is illustrated on figure 4 for $k = 0$ (c) and $k = 1$ (d), and these elements will respectively be named NC_5 and NC_{12} in the remainder of this paper. This yields a non-conforming scheme since continuity of the flux is not enforced across element interfaces.

The spatially and angularly discretized form of Ψ^+ is then given by

$$\Psi^+(\boldsymbol{r}, \boldsymbol{\Omega}) \approx (y_e(\boldsymbol{\Omega}) \otimes f(\boldsymbol{r}))\, \varphi_+, \tag{15}$$

where φ_+ is the coefficient column vector to be determined, y_e contains the even-parity spherical harmonics as before, and where $f(\boldsymbol{r})$ contains the basis functions spanning $Q_{k+2,k} \cup Q_{k,k+2}$. Taking test functions equal to the (transposed) expansion functions, and substituting equation (15) into the weak form given by equation (13), yields a positive-definite system that can be solved using powerful iterative techniques such as preconditioned conjugate gradients (Saad 2003).

With this approach, we come close to the reference solution for the fixed-source test problem introduced in Section 3.2, as can be seen on figure 3 (line of "$*$"). To further demonstrate the convergence of the NC_5 and NC_{12} elements, table 1 gives the root mean square (or L^2) error norm for different mesh refinements. Such a good result was not guaranteed a priori. In fact, the convergence of

	L^2 error norm, $\times 10^4$			
type \ grid	5×5	10×10	20×20	40×40
NC_5	695.2	5.3	3.9	2.4
NC_{12}	684.0	13.4	4.6	2.2
NC_4	702.0	20.9	7.0	2.9
NC_4^*	719.3	47.1	12.4	3.7

Table 1
L^2 error norm (on the cell-averaged flux values, compared to the reference IDT calculation obtained on a 40×40 grid) for different mesh refinements, using a P_5 angular approximation.

a non-conforming scheme is often theoretically investigated through a "patch test" (Strang and Fix 1973), whose mathematical foundations lie in the second Strang lemma (Ciarlet 1978). This patch test is not passed here (the continuity of the mean value is not guaranteed across element interfaces), but nevertheless the results obtained are good. Moreover, one can argue that the "patch test" was developed for simple second-order partial differential equations (typically $-\Delta u = f$) and is thus not directly applicable in the more general case of the transport equation.

A simple low-order element can be obtained by removing the interior degree of freedom in the NC_5 element. We then obtain a rectangular element with one node on the middle of each side. The basis $\{1, x, y, xy\}$ is not unisolvent with such node positioning, and the spatial basis to use is then $\{1, x, y, x^2 - y^2\}$. This element will be named NC_4 in this paper. Note that this element can be obtained by simply rotating the usual lowest-order Lagrangian element. In fact, it is known as the "rotated Q_1" element in the numerical analysis community. It was tested long ago by Lautard (1981) on the diffusion equation, and more recently used by Rannacher and Turek (Rannacher and Turek 1992) for the Stokes problem. Again the patch test is not passed for this element, but our test problem was successfully treated by this approach. The L^2 error norm evolution with mesh refinement is also given in table 1.

The NC_4 element has been further analyzed by Douglas et al. (1999) for general second-order elliptic problems. Following their suggestion, we can replace the basis $\{1, x, y, x^2 - y^2\}$ by $\{1, x, y, \theta(x)^2 - \theta(y)^2\}$ with

$$\theta(x) = x^2 - \frac{5}{3}x^4.$$

With the reference element defined as $[-1, 1]^2$, and since $\int_{-1}^{1} \theta(x) = 0$, this basis insures that the average flux is continuous across each element side. The resulting element will be denoted by NC_4^*. The patch test at order zero is thus passed for this element. Again, the NC_4^* element was validated on our fixed-source test problem, and table 1 gives the L^2 error norm evolution.

5 Criticality calculations

Criticality calculations have been performed to further test the non-conforming finite elements validated in the previous section. A two-dimensional adaptation of the Takeda 1 benchmark (Takeda et al. 1989) was used. Its geometry is described in figure 5 and its cross-sections are summarized in table 2. A simplified whole core is represented, and the cross-section values correspond to a case were the control rods are absent (this is to make the test more severe). A

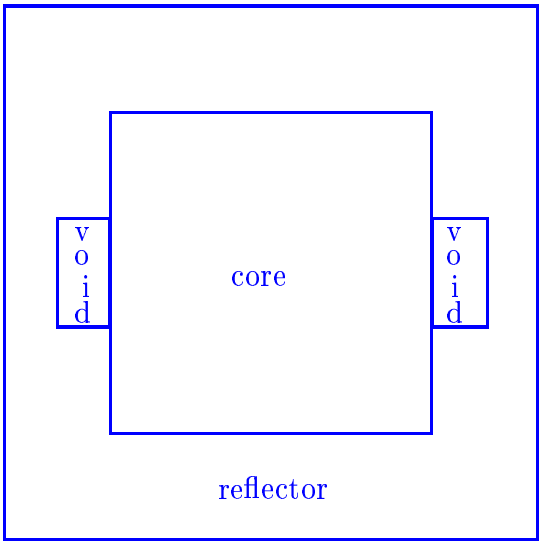

Fig. 5. Geometry for the 2-D Takeda 1 benchmark without control rod. Vacuum boudaries are considered on each edge

region	group	σ_t	$\nu\sigma_f$	σ_s	
				from group 1	from group 2
core	1	0.223775	0.00909319	0.192423	0.0
	2	1.03864	0.290183	0.0228253	0.880439
reflector	1	0.250367	0.0	0.193446	0.0
	2	1.64482	0.0	0.0565042	1.62452
void	1	0.0128407	0.0	0.01277	0.0
	2	0.0120676	0.0	2.40997E-05	0.0107387

Table 2
Cross-section values for the 2-D Takeda 1 benchmark. The fission spectrum χ is taken equal to 1 in group 1 and 0 in group 2.

reference S_{12} discrete ordinate calculation for this benchmark was performed using an 80×80 grid, yielding a $k_{eff} = 1.12971$. The same value was obtained with a 40×40 grid. As expected, the SP_N solver MINOS did not reproduce the reference solution. Moreover, the MINOS solver failed to provide a converged value, even with 50 inner iterations (while only one inner iteration is usually sufficient for not so severe tests). It thus seems that not only the discretization

scheme but also the numerical solution scheme of MINOS is not appropriate to treat this benchmark.

The new P_N solver uses the standard power iteration method for the outer iteration with Tchebyshev acceleration. For the inner iteration, it uses a preconditioned conjugate gradient algorithm, where the preconditioning is done by forward-backward Gauss-Seidel or incomplete Cholesky factorization.

The proposed non-conforming schemes, that were proved appropriate for the fixed-source problem, also appear appropriate on this criticality problem. This can be seen in tables 3 and 4.

	P_1		P_3	
grid / type	40×40	80×80	40×40	80×80
NC_5	1.10664	1.10636	1.12807	1.12783
NC_{12}	1.10623	1.10617	1.12757	1.12758
NC_4	1.10673	1.10637	1.12798	1.12777
NC_4^*	1.10744	1.10649	1.12895	1.12797
LL_4	1.10727	1.10639	1.12909	1.12799
PL_9	1.10611	1.10613	1.12765	1.12759
CL_{16}	1.10612	1.10613	1.12758	1.12758

Table 3
k_{eff} values obtained with the proposed non-conforming elements, as well as with linear (LL4), parabolic (PL9) and cubic (CL16) Lagrangian elements.

These tables also show the results obtained with the same second-order primal formulation, but using the usual Lagrangian elements (e.g. R.T.Ackroyd 1997). With all our second-order schemes, increasing the P_N order yields k_{eff} values that come increasingly closer to the reference S_{12} solution. To examine more closely the performances of the various schemes, the most appropriate test is to take as reference, for each angular order N, the corresponding cubic Lagrangian (CL_{16}) result (we are certain of the convergence of the conforming elements). As could be expected, the NC_{12} element is much more precise than the NC_5 element. Also, as all our NC schemes, the NC_4 element provide better results than the LL_4 element, especially on the coarser mesh. The fact that the NC_4 element is often more precise than the NC_5 one might be fortuitous.

With the P_5 approximation, figures 6 and 7 respectively show the Δk_{eff} and the root mean square $\|\Delta P\|_2$ of the error on the power versus the total num-

	P_5		P_7	
grid / type	40×40	80×80	40×40	80×80
NC_5	1.12960	1.12909	1.13043	1.12958
NC_{12}	1.12867	1.12871	1.12902	1.12905
NC_4	1.12910	1.12885	1.12941	1.12920
NC_4^*	1.13012	1.12915	1.13047	1.12953
LL_4	1.13028	1.12918	1.13065	1.12957
PL_9	1.12885	1.12875	1.12924	1.12912
CL_{16}	1.12875	1.12873	1.12911	1.12909

Table 4
k_{eff} values obtained with the proposed non-conforming elements, as well as with Lagrangian elements (Continued).

ber of non-zero system matrix elements. This emphasizes the additional cost required to achieve greater precision. Note that while the NC_4 element performs better than the NC_4^* element in terms of k_{eff}, the opposite is true for the power.

Table 5 further illustrates the cost of each of the second-order schemes in the P_5 case. Beside the number of unknowns and off-diagonal elements in the system matrix, this table gives the computing time needed using a forward-backward Gauss-Seidel preconditioning for all schemes. The C++ code used to implement the method was not optimized for computational efficiency. Therefore it is not appropriate to compare the execution times against other computer programs. However, since the different methods have been programmed the same way, comparing their CPU times is relevant. This comparison reveals that the computing time is roughly directly proportional to the number of non-zero elements in the system matrix.

Table 5 presents estimates of the condition number of the global matrix. The condition number of a matrix is the ratio of the largest to the smallest eigenvalue. A value close to unity indicates a better conditioned matrix (Saad 2003). We notice that the condition number with NC_4 is almost as good as the one with LL_4. Note that neither the Lagrangian nor the non-conforming schemes yield a diagonally dominant matrix or an M-matrix (Saad 2003) (known to have good preconditioning capabilities) in the general P_N case. Another estimate of the conditioning of the matrix is the bandwidth size, since this size limits the fill-in when using (complete or incomplete) Cholesky factorization techniques. The average bandwidth values are also given in table 5.

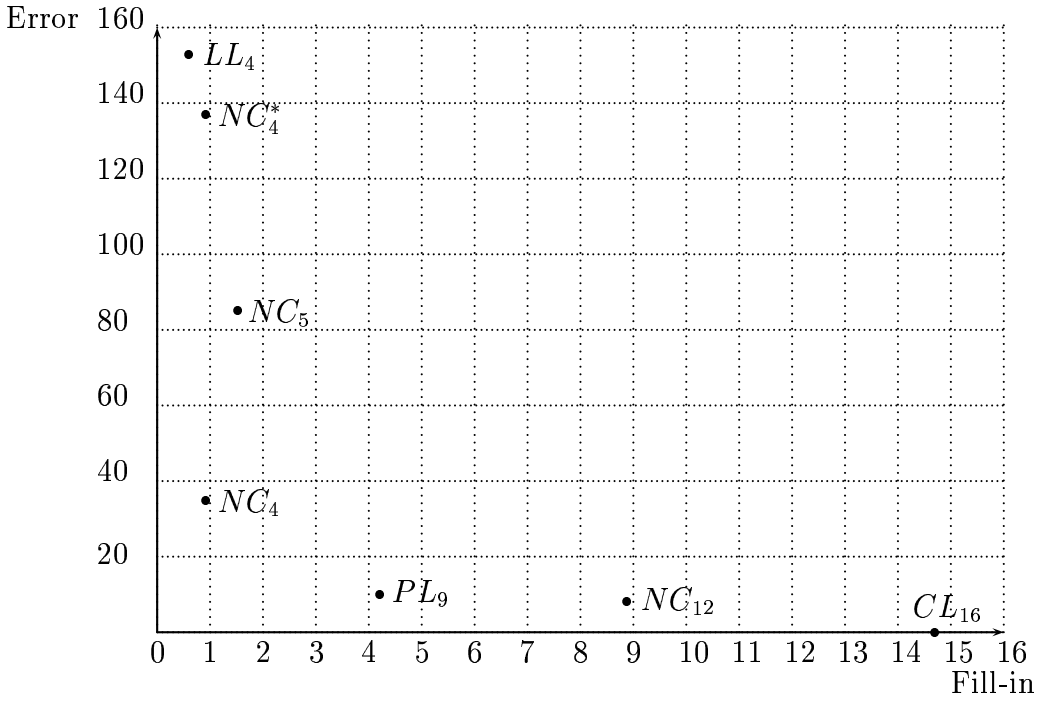

Fig. 6. Δk_{eff} (in pcm, with CL_{16} taken as reference) versus fill-in (number of nonzero elements in the system matrix, in millions) for the 2-D Takeda 1 benchmark without control rod.

6 Conclusions

We first investigated the introduction of a vector unknown into the mixed-dual formulation of the transport equation obtained through the even/odd parity decomposition. A heuristically motivated extension of the RT element was proposed to discretize the resulting formulation. Unfortunately, this approach failed to provide acceptable results on a demanding test problem. Other schemes introducing a vector and a scalar unknown could possibly be developed. However, it is doubtful that such scheme would remain simple and in turn applicable in practice. One should moreover remember that mixed methods were primarily introduced to obtain an approximation of the vector unknown directly, that is avoiding errors in the differentiation of the scalar unknown. However, in the typical criticality calculation context, the vector unknown $\boldsymbol{J}$ is not needed. In fact, the reason why mixed methods perform well in the diffusion (and SP_N) case is not known. The solution method (i.e., the ADI in the case of the MINOS solver) plays a key role in the efficiency of the solver, but from a purely discretization point of view, no theoretical result show the superiority (in terms of conditioning) of the mixed linear system compared to the second-order one. An obvious observation can however be made, that is that the introduction of the current unknown increases the size

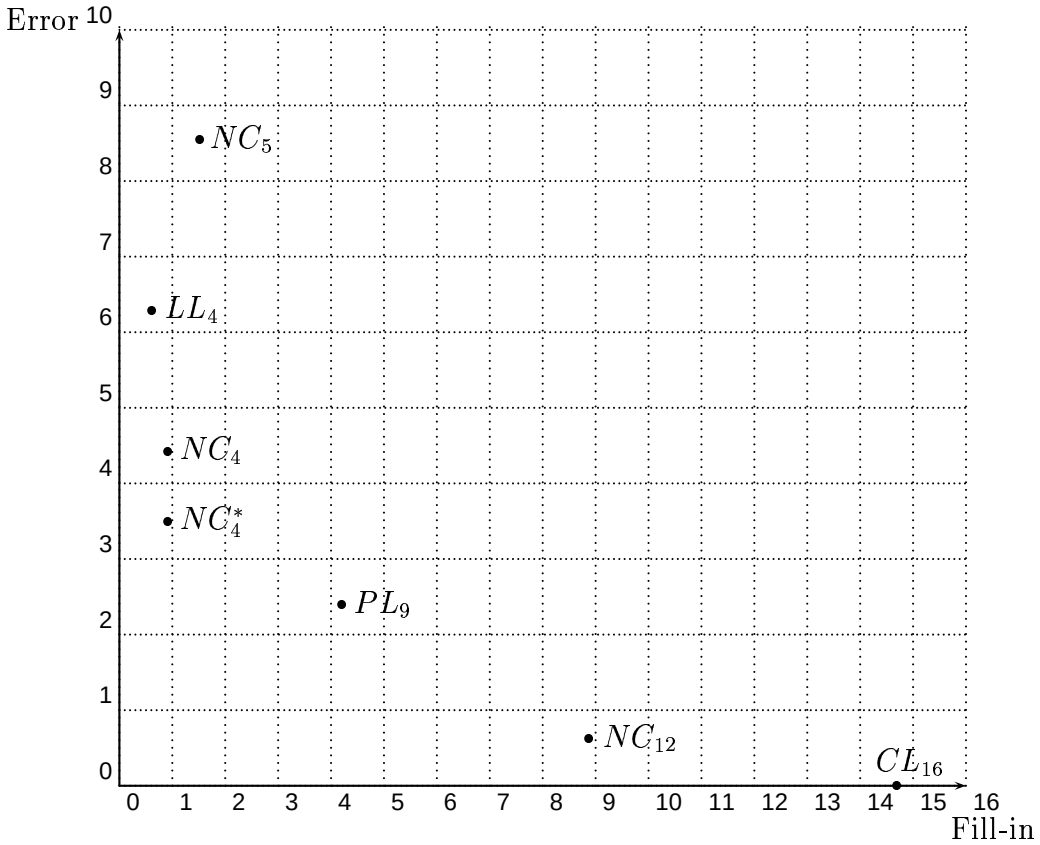

Fig. 7. L_2 error norm ($\times 1000$, with CL_{16} taken as reference) versus fill-in (number of nonzero elements in the system matrix, in millions) for the 2-D Takeda 1 benchmark without control rod.

of the discretized system to be solved. It is interesting to note that recovery techniques (Chou et al. 2002) have been developed by numerical analysts to efficiently re-construct the vector unknown from the scalar one, once the latter has been obtained through a non-conforming scheme. Such techniques rely on the equivalence between the non-conforming scheme and the mixed one, and actually claim to take advantage of the lower dimension of the system arising from the non-conforming scheme. Thus in our case, where the vector unknown is in fact useless, the use of mixed methods may seem to be an unnecessarily complicated way to proceed.

We here adapted Hennart's approach to the transport case with P_N angular approximation, introducing a family of 2-D non-conforming finite elements whose lowest two order elements have been denoted NC_5 and NC_{12}. These elements were shown to yield satisfying results on a severe fixed-source test problem, as well as on a similar criticality calculation. Such convergence was not guaranteed a priori (the patch test is not passed for these elements). Further simplifying the lowest-order non-conforming element by eliminating the interior degree of freedom lead to the NC_4 (or rotated Q_1) non-conforming element. We showed that this element is also convergent on our severe test

type	# unknowns	# off-diag	CPU time	cond. number	bandwidth
NC_5	43,920	1,471,680	89.95	392.39	724
NC_{12}	116,640	8,767,440	975.9	1219.5	1,808.5
NC_4	29,520	895,680	51.04	83.17	544
NC_4^*	29,520	895,680	51.44	183.57	544
LL_4	15,129	585,396	29.45	67.44	373
PL_9	59,049	4,143,636	282.6	647.98	1,097
CL_{16}	131,769	14,562,756	1,037.22	2044.1	2,182

Table 5
Various measures of cost and conditioning for a P_5 calculation using a 40×40 grid: number of unknowns and number of off-diagonal non-zero elements in the system matrix, CPU time (in seconds), condition number (on a reference 8×8 calculation) and average bandwidth.

problem.

The question is then to see whether or not the non-conforming schemes we consider do add significant improvement compared to the Lagrangian ones used in (de Oliveira 1986), for instance. Numerical results in Section 5 show that the family NC_5, NC_{12},... is clearly more costly than the Lagrangian one and that this additional cost is not always compensated by an equivalent increase in accuracy. However, the NC_4 element is potentially interesting, since it yields an improved accuracy compared to LL_4, sometimes close to PL_9 but at a lower cost. Relatively recent research about this element, including 3-D generalization has been performed in other fields (Douglas et al. 1999). This will be the subject of further research. Note also that the triangular equivalent of the NC_4 element exists in the literature under the name of Crouzeix-Raviart element (Crouzeix and Raviart 1973). It would be interesting to couple these two non-conforming elements together to treat various geometries. Also, experience with nodal methods lead us to think that the relaxation of the interface continuity constraint should make non-conforming schemes particularly efficient where a coarser mesh can be used. One could then think about coupling non-conforming elements with conforming Lagrangian ones, each of them being used in selected areas.

For solving the linear system resulting from the non-conforming scheme, a preconditioned conjugate gradient method has been used in this study. Multilevel methods for non-conforming elements have been studied in the numerical analysis community (Chen 1997; Chen and Oswald 1998). This will also be the subject of further work.

Acknowledgments

The author acknowledges J.-J. Lautard, A.-M. Baudron and F. Moreau for many helpful discussions. The author also acknowledges Igor Zmijarevic for providing the IDT numerical results presented in Fig. 3.

References

Arbogast, T. and Z. Chen (1995). On the implementation of mixed methods as nonconforming methods for second order elliptic problems. *Math. Comp. 64*, 943–972.

Arnold, D. and F. Brezzi (1985). Mixed and non conforming finite element methods: implementation, postprocessing and error estimates. *Math.Mod.Numer.Anal. 19*(1), 7–32.

Azmy, Y. (1987, 27-30 April). Multidimensional linear-linear nodal transport methods in weighted diamond difference form. In *Proceeding of the International Topical Meeting on advances in reactor physics, mathematics and computation*, Paris, pp. 1005–1019.

Baudron, A. and J. Lautard (2005, Sept. 12-15). Minos : A SP_N solver for core calculation in the descartes system. In *Proc. International Topical Meeting on Mathematics and Computation, Supercomputing, Reactor Physics and Nuclear and Biological Applications*, Avignon, France.

Cartier, J. (2005a). private communication.

Cartier, J. (2005b, Sept. 12-15). Mixed and hybrid finite element method for the transport equation. In *Proc. Int. Conf. Mathematics and Computation, Supercomputing, Reactor Physics and Nuclear and biological Applications*, Avignon, France.

Chen, Z. (1997). The analysis of intergrid transfer operators and multigrid methods for nonconforming finite elements. *Electronic Transactions on Numerical Analysis 6*, 78–96.

Chen, Z. and P. Oswald (1998). Multigrid and multilevel methods for nonconforming Q_1 elements. *Math. Comp. 67*, 667–693.

Chou, S., D. Kwak, and K. Kim (2002). Flux recovery from primal hybrid

finite element methods. *SIAM J. Numer Anal. 40*(2), 403–415.

Ciarlet, P. (1978). *The Finite Element Method for Elliptic Problems*. Studies in Mathematics and its Applications. Amsterdam: North Holland.

Crouzeix, M. and P. Raviart (Decembre 1973). Conforming and nonconforming finite element methods for solving stationary stokes equations. *RAIRO-3 Analyse numérique*, 77–104.

de Oliveira, C. (1986). An arbitrary geometry finite element method for multigroup neutron transport with anisotropic scattering. *Progress in Nuclear Energy 18*(1/2), 227–236.

del Valle, E. and E. Mund (2004). RTk/S_N solutions of the two-dimensional multigroup transport equations in hexagonal geometry. *Nuclear Science and Engineering 148*(1), 172–185.

Douglas, J., J. Santos, D. Sheen, and X. Ye (1999). Nonconforming galerkin methods based on quadrilateral element for second order elliptic problems. *Mathematical Modelling and Numerical Analysis 33*(4), 747–770.

Fedon-Magnaud, C., J. Lautard, B. Akherraz, and G. Wu (April 30 - May 4, 1995). Coarse mesh methods for the transport calculation in the cronos reactor code. In *Proc. Int. Conf. Math, Comp, Reactor Physics and Environmental Analysis of Nuclear System*, Portland, Oregon, pp. 508–526.

Ha, T., J. Santos, and D. Sheen (2002). Nonconforming finite element methods for the simulation of waves in viscoelastic solids. *Comput. Methods Appl. Mech. Engrg. 191*, 5647–5670.

Hennart, J. (1986). A general family of nodal schemes. *SIAM J. Sci. Stat. Comput. 7*(1), 264–286.

Hennart, J. and E. del Valle (1993). On the relationship between nodal schemes and mixed-hybrid finite elements. *Numer.Methods Partial Different Eqs 9*, 411.

Kloucek, P., B. Li, and M. Luskin (1996). Analysis of a class of nonconforming finite elements for crystalline microstructures. *Math. Comp. 65*(215), 1111–1135.

Lautard, J. (1981, April 27-29). New finite element representation for 3D reactor calculations. In *Proc. of the Topical Meeting on Advances in Mathematical Methods for the Solution of Nuclear Engineering Problems*, Munchen, Germany.

Lautard, J., D. Schneider, and A. Baudron (1999, Sept. 27-30). Mixed dual methods for neutronic reactor core calculations in the CRONOS system. In *Proc. Int. Conf. Mathematics and Computation, Reactor Physics and Environmental Analysis of Nuclear Systems*, Madrid, Spain, pp. 814–826.

Morel, J. and J. McGhee (1999). A self-adjoint angular flux equation. *Nuclear Science and Engineering 132*, 312–325.

Palmiotti, G., E. Lewis, and C. Carrico (1995). VARIANT: VARIational Anisotropic Nodal Transport for multidimensional cartesian and hexagonal geometry calculations. Technical Report ANL-95/40, Argonne National Laboratory.

Rannacher, R. and S. Turek (1992). Simple nonconforming quadrilateral stokes element. *Numerical Methods for Partial Differential Equations 8*, 97–111.

Raviart, P. and J. Thomas (1977). A mixed finite element method for second-order elliptic problems. In *Mathematical aspects of the finite element method*, Volume 606 of *Lecture Notes in Mathematics*, Berlin, pp. 292–315. Springer-Verlag.

Roberts, J. and J.-M. Thomas (1991). Mixed and hybrid methods. In P.G.Ciarlet and J.L.Lions (Eds.), *Handbook of Numerical Analysis*, Volume 2, pp. 523–633. Amsterdam: North Holland.

R.T.Ackroyd (1997). *Finite Element Methods for Particle Transport*. John Wiley and Sons.

Saad, Y. (2003). *Iterative Methods for Sparse Linear Systems*. SIAM.

Strang, G. and G. Fix (1973). *An Analysis of the Finite Element Method*. Prentice-Hall.

Takeda, T., M. Tamitani, and H. Unesaki (1989). Proposal of 3D neutron transport benchmark. NEACRPA-953 rev.1, Department of nuclear engineering, Osaka University, Japan.

Van Criekingen, S. (2004). *Mixed-hybrid discretization methods for the linear transport equation*. Ph. D. thesis, Northwestern University, Evanston, IL, USA.

Van Criekingen, S., E. Lewis, and R. Beauwens (2006). Mixed-hybrid transport discretization using even and odd P_N expansions. *Nuclear Science*

and Engineering 152(2), 149–163.

Vladimirov, V. (1963). Mathematical problems in the one-velocity theory of particle transport. Technical report, Atomic Energy of Canada Ltd., Ontario. translated from Transactions of the V.A. Steklov Mathematical Institute, **61**, 1961.

Wu, G. (1996). *Application de la méthode mixte duale à la résolution des équations de la diffusion et du transport*. Ph. D. thesis, Université Paris XI Orsay, Orsay, France.

Zmijarevic, I. (1999, Sept. 27-30). Multidimensional discrete ordinates nodal and characteristics methods for the APOLLO2 code. In *Proc. Int. Conf. Mathematics and Computation, Reactor Physics and Environmental Analysis of Nuclear Systems*, Madrid, Spain, pp. 1587–1597.